Available online at www.sciencedirect.com
ScienceDirect
Antiviral Research 77 (2008) 83–94
Antiviral Research
www.elsevier.com/locate/antiviral

Inhibition of human parainfluenza virus type 3 infection by novel small molecules

Hongxia Mao [a], Chandar S. Thakur [b], Santanu Chattopadhyay [a], Robert H. Silverman [b], Andrei Gudkov [a], Amiya K. Banerjee [a,*]

[a] *Department of Molecular Genetics, Virology Section NN10, Lerner Research Institute, Cleveland Clinic Foundation, 9500 Euclid Avenue, Cleveland, OH 44195, USA*
[b] *Department of Cancer Biology, Lerner Research Institute, Cleveland Clinic Foundation, 9500 Euclid Avenue, Cleveland, OH 44195, USA*

Received 14 May 2007; accepted 4 September 2007

Abstract

Human parainfluenza virus type 3 (HPIV3) is an important respiratory tract pathogen of infants and children. There are no vaccines or antivirals currently approved for prevention or treatment of HPIV3 infection. Towards developing an antiviral therapy to combat HPIV3 infection, we have established a green fluorescent protein (GFP)-tagged HPIV3 infected-cell assay and used it for screening of a small molecule library obtained from ChemBridge Diver. Two novel small molecules (C5 and C7) which shared structural similarities were identified and their inhibitory effects on HPIV3 were confirmed in CV-1 and human lung epithelium A549 cells by plaque assay, Western blot and Northern blot analyses. C5 and C7 effectively prevented the cytopathic effect in cells infected with HPIV3, achieving IC_{50} values of 2.36 μM and 0.08 μM, respectively, for infectious virus production. The inhibition appears to be at the primary transcriptional level of HPIV3 life cycle based on sequential time course test, binding and internalization assays, and finally by a minigenome transcription assay in cells as well as measuring viral transcripts in cells in the presence of anisomycin. Interestingly, vesicular stomatitis virus (VSV), another member of mononegavirales order, was also inhibited by these compounds, whereas poliovirus–a picornavirus was not. Use of these inhibitors has a strong potential to develop novel antiviral agents against this important human pathogen.

Keywords: HPIV3; Small molecules; Primary transcription; Mononegavirales

1. Introduction

Human parainfluenza virus (HPIV3), a member of paramyxoviridae family is a respiratory pathogen affecting children worldwide causing croup, bronchiolitis, and pneumonia (Moscona, 2005; Reed et al., 1997). It is second only to respiratory syncytial virus (RSV) resulting in acute respiratory infections that require hospitalization of infants and children (Heilman, 1990; Murphy, 1988). It is also an important cause of morbidity and occasional mortality in immunocompromised patients, especially for those undergoing allogeneic hematopoietic stem cell transplantation (Cortez et al., 2001; Madhi et al., 2002).

HPIV3 is a single-stranded, nonsegmented, negative strand RNA virus. Its 15,462 base genomic RNA of negative polarity contains a 3′ leader RNA complement of 55 nucleotides, a 5′ trailer RNA of 44 nucleotides and the six genes of N, P, M, F, HN, and L flanked between these two *cis*-regulatory regions. The junction connecting two genes includes conserved gene-end, intergenic (IG) and gene-start sequences. These genes are transcribed sequentially into mRNAs by the virion-associated RNA polymerase consisting of a large protein (L) and a phosphoprotein (P). During infection, HPIV3 binds to the target cells, via interaction of the viral glycoprotein HN with sialic acid containing receptor molecules on the cell surface (Bose and Banerjee, 2002). The envelope then fuses directly with the plasma membrane of the cell, mediated by the viral fusion protein (F protein), releasing the nucleocapsid (RNP) into the cytoplasm (Moscona, 2005). In the cytoplasm, the viral polymerase (P–L) transcribes (primary transcription) the N-encapsidated genome RNA (N:RNA), starting from the 3′ end, to generate the (+) leader RNA and the successive capped and polyadenylated mRNAs, by terminating and reinitiating at each gene junction. Once sufficient unassembled N (as a P–N complex) is generated,

* Corresponding author. Tel.: +1 216 444 0625; fax: +1 216 444 2998.
E-mail address: banerja@ccf.org (A.K. Banerjee).

0166-3542/$ – see front matter © 2007 Elsevier B.V. All rights reserved.
doi:10.1016/j.antiviral.2007.09.001

the viral polymerase then ignores all gene junctions and produce an antigenome RNA into a fully assembled nucleocapsid, by coordinated RNA synthesis and encapsidation (Lamb and Kolakofsky, 1995). Genome synthesis from antigenome template occurs in a fashion similar to that of antigenome synthesis. The nucleocapsid of the virus is subsequently assembled in the cytoplasm and virus buds from the apical surface of the epithelial cells (Bose et al., 2001).

Currently, there are no vaccines or antivirals approved for the prevention and treatment of HPIV3 infection. Although the HPIV3 candidate vaccine cp45 (Belshe et al., 2004) was shown to be safe and immunogenic in young children in phase I and II trials, it still needs to be evaluated in phase III efficacy studies. Clinical evaluation of bovine/human PIV3 chimeras, another attractive HPIV3 candidate vaccine, is at the early stage of development (Durbin and Karron, 2003). Antiviral therapy to combat this virus has not been systematically carried out (Alymova et al., 2004; Pastey et al., 2000; Tanaka et al., 2006). Our laboratory has been actively involved in developing such potential antiviral compounds towards this important human pathogen. Here, we screened 3600 compounds from a chemical library containing 34,000 novel small molecules (molecular weight 250–550) for potential antiviral agent(s) by using recombinant GFP-tagged HPIV3 (r-GFP-HPIV3) infected cell assay. We obtained two compounds (C5 and C7) with the IC_{50} of 2.36 μM and 0.08 μM, respectively. Further studies suggest that the compounds inhibit viral replication at the primary transcriptional level.

2. Materials and methods

2.1. Cells and viruses

Human cervix adenocarcinoma cells (HeLa), Africa green monkey kidney cells (CV-1) and human lung carcinoma cells (A549) were cultured in Dulbecco's Modified Eagle Medium (DMEM) containing glutamine, penicillin and streptomycin supplemented with 10% fetal bovine serum. HPIV3 (HA-1; NIH 47885) and Vesicular Stomatitis Virus (VSV) were grown in CV-1 cells. Poliovirus was generously supplied by Dr. Nickolay Neznanov (Neznanov et al., 2005) and grown in HeLa cells.

2.2. Chemicals

Chemicals for screening (about 34,000) were from CamBridge Diverset library. The compounds C5 and C7 were purchased from the CamBridge Corp. at 5 mg scale. Stock solutions were prepared by dissolving chemicals in 100% DMSO and were stored at −20 °C.

2.3. Plasmid construction

The infectious cDNA clone pHPIV3 (Hoffman and Banerjee, 1997) was digested with PmlI and XhoI, and the resulting fragment containing virus bases from 1213 to 7443 was inserted into the same site in pUC119 introduced by the method of Kunkel (Kunkel, 1985). The virus genome bases 3700–3705 (TCAATC) in the pUC119-F1213-7443 were mutated to AflII site (CTTAAG) by the same method. PCR product encompassing GFP was generated from pGEM4-GFP by using a pair of primers containing AflII site (underlined): GFP3700AflIIs/5′-gccCTTAAGAATATACAAATAAGAAAAATTTAGGATTA-AAG agcg*ATGGTGAGCAAGGGCGAGGAGCTGTTCACCG-GG*-3′, and GFP3700AflIIa/5′-gccCTTAAG TTATTCGGTGT-TGTTTTTTTTATTTGATCT *CTACTTGTACAGCTCGTCCA-TGCCGAGAGTGATCCC*-3′. GFP3700AflIIs also encodes P end (3706–3724), Intergenic (IG) TTT, and M start (3728–3737) at the upstream of GFP initial sequence (in italic), and GFP3700AflIIa also encodes P end (3599–3628) at upstream of GFP end sequence (in italic). GFP PCR product was cloned into the AflII site in pUC119-F1213-7443. The GFP clone in a pUC119 background was then digested with RsrII and XhoI, and the resulting fragment was inserted into the same site in pOCUS-HPIV3. This generated pOCUS-HPIV3-GFP, the infectious clone with GFP encoding sequence inserted between P and M genes.

2.4. Recovery of recombinant GFP-tagged HPIV3 (r-GFP-HPIV3)

r-GFP-HPIV3 was recovered as described previously (Hoffman and Banerjee, 1997). In brief, the monolayer of HeLa cells was infected with recombinant vaccinia virus vTF7-3 which expresses T7 RNA polymerase at a multiplicity of infection (MOI) of 2. After 1 h at 37 °C, pOCUS-HPIV3-GFP (0.5 μg) was transfected along with plasmids encoding the HPIV3 proteins NP (1 μg), P (2 μg) and L (0.05 μg) into the HeLa cells by using Lipofectin (Invitrogen). The cultures were incubated at 37 °C for 3 h, then the medium was replaced with fresh DMEM containing 5% fetal bovine serum. After incubation at 37 °C for an additional 2 days, the plates were frozen, thawed and scraped, and the cell supernatant was harvested by centrifugation at 10,000 rpm for 5 min at 4 °C. The clarified supernatant was layered onto fresh HeLa monolayers once, subsequently on fresh CV-1 monolayers in the presence of 25 μg/ml 1-β-D-arabinofuranosylcytosine (Ara-C) to inhibit vaccinia virus replication. The single recovered r-GFP-HPIV3 was isolated by picking up as agar plugs during titering and further amplified by passage in CV-1 cells. Photographs of r-GFP-HPIV3 infected cells were taken with a Leica inverted fluorescence microscope equipped with a digital camera.

2.5. Screening of the small molecule library by using the r-GFP-HPIV3 infected CV-1 cell-based system

To evaluate the r-GFP-HPIV3 infected CV-1 cell based system, the CV-1 cells were treated with IFN-α at concentrations of 10 u/ml, 100 u/ml, and 1000 u/ml overnight (16 h) as described previously (Gao et al., 2001) and subsequently infected with r-GFP-HPIV3 at an MOI of 1 for a maximum of GFP expression. At 24 h post-infection (PI), the GFP expression in infected cells was observed under fluorescence microscope. The screening process is as follows: Four to 5×10^4 CV-1 cells were seeded into 96-well plates the day before infection with one well per plate being treated with 1000 u/ml of IFN-α overnight (16 h)

as a positive control. On the next day, the media from each well were replaced with 200 μl of Opti-MEM. Then compounds (13.7 mM in DMSO) were added into media at 0.2 μl/well and the final concentrations were 13.7 μM. After 1 h, 10 μl of r-GFP-HPIV3 (4×10^6 pfu/ml) were added to infect cells in each well at an MOI of 1. At 24 h PI, the media were removed and the fluorescence in cells of each well was quantified at excitation/emission wavelength of 485/535 nm with a VICTOR Readout System (Wallac VICTOR$^2{}_{TM}$, 1420 MULTILABLE COUNTER, Perkin-Elmer^{TM}). Blue staining assay was further performed to reflect the cytotoxicity of compounds. In brief, 50 μl of 1% MeBlue, 50% methanol was added into wells and kept for 5–10 min. The wells were washed with water for three times and air-dried for 20 min. After that, 50–100 μl of 1% SDS (in phosphate-buffered saline (PBS)) was added and the plates were scanned at 600 nm. The Ab600 values were used to estimate the cytotoxicity of compounds. The primary "hits" were identified as the compounds which decreased the fluorescence in cells to background level in non-infected cells or in IFN-α-treated infected cells while keeping similar blue staining values.

2.6. Plaque assay

The virus titer was determined by plaque assay as described previously (Choudhary et al., 2001). Briefly, the virus sample (or clarified supernatant) was serially diluted in 1 ml of Opti-MEM to 10^{-4}, 10^{-5}, and 10^{-6} or 10^{-5}, 10^{-6}, and 10^{-7}. Confluent monolayers of CV-1 cells in 6-well plates were washed with PBS and incubated with the diluted suspension at 37 °C, 5%CO_2 for 1.5 h. The media was removed and cells were washed with PBS and overlaid with 0.8% methyl cellulose (in 1 × MEM, containing 5% fetal bovine serum, 2 mM L-glutamine, 15 mM hepes buffer, 0.075% NaHCO3, 5 mM NaOH, 2.5 μg/ml Fungizone, 0.2 mg/ml Gentamicin). After 48 h, the methyl cellulose was aspirated and cells were stained with 1% crystal violet (in 50% methanol). Plaques were counted and the average number of plaques in duplicate wells was used to determine the titer of the virus sample. The IC_{50} is defined as the 50% inhibitory concentration for virus yield detected by plaque assay. EC_{50} is 50% effective concentration.

2.7. Western blot

Western blot was performed by standard protocols as previously described (Yuan et al., 2004) with some modification. The clarified supernatant was mixed with equal volume of 2 × SDS gel-loading buffer (100 mM Tris–Cl PH 6.8, 4% SDS, 0.2% bromophenol blue, 20% glycerol, and 200 mM dithiothreitol) and heated at 95 °C for 5 min. Twenty-five microliters of each sample was subjected to 10% sodium dodecyl sulfate-polyacrylamide gel electrophoresis (SDS-PAGE) and then transferred to nitrocellulose membrane (BioRad, Transfer-Blot®) at 100 V for 45 min at 4 °C. After blocking with 5% nonfat milk (in PBS containing 0.1% tween 20) for 1 h, the membrane was probed with monoclonal anti-HN of HPIV3 (Fitzgerald, clone# M02122321, 2.0 mg/ml, 1:1000 dilution) or anti-GAPDH (Santa Cruz Biotechnology, Sc-32233, 200 μg/ml, 1:2000 dilution) at 4 °C overnight followed by incubation with horseradish peroxidase-conjugated goat anti-mouse IgG (Santa Cruz Biotechnology, Sc-2005, 200 μg/0.5 ml, 1:1000 dilution) at room temperature for 1 h. Finally, HN or GAPDH expression was detected by ECL reagents (Amersham Biosciences).

2.8. Northern blot

Northern blot was performed by standard protocols as previously described (Mansfield et al., 1999) with some modifications. In brief, the total RNA was extracted by using Trizol® reagent (Invitrogen) according to the manufacturer's instruction. Five or 15 μg of total RNA for each sample were subjected to 1.2% Agarose gel containing 18% formaldehyde and then capillary transferred to Immobilon^{TM}-Ny$^+$ membrane (MilliPore). The blots were air-dried completely and then exposed to a UV light source (254 nm) equipped in Stratalinker (Stratagen) for RNA fixation. The total exposure energy was 20,000 microJoules/cm^2. The ^{32}P labeled probes of NP or GAPDH were made by using random primed DNA labeling kit (Roche) and purified with Quick Spin Column (Roche). Pre-hybridization and hybridization were performed at 68 °C in hybridization buffer (0.5 M sodium phosphate PH 7.1, 2 mM EDTA, 7% SDS, 0.1% sodium pyrophosphate). After washing with Wash buffer I (1 × SSPE, 0.1% SDS) and Wash buffer II (0.2 × SSPE, 0.1% SDS), the blots were wrapped and exposed to autoradiographic film for radioactive detection. Stripping of blots for re-probing was performed in the stripping solution (0.1% SDS) according to the Transfer Membrane User Guide of Millipore. The individual bands were quantified using Image-Quant 5.2.

2.9. Cell viability assay

Cell viability/cytotoxicity of compounds was determined using a 3-(4,5-dimethylthiazolyl-2)-2,5-diphenyltetrazolium bromide (MTT) cell proliferation assay kit (ATCC). Cells in 96-well plates (5×10^4/well) were treated with various concentrations of compounds for 24 h, 48 h or 72 h. Then cells were incubated with 20 μl MTT reagent for 2–3 h. One hundred microliters of detergent reagent were added and the plate was left at room temperature in the dark for 2 h. The absorbance in each well was read at 560 nm with the VICTOR Readout System. The values for each sample were determined by subtracting the average absorbance of the media-only blanks from its average triplicate reading. The cell viability for each sample is represented as a percentage of the average value of non-infected cells.

2.10. ^{35}S-HPIV3 adsorption and internalization assay

[^{35}S] Methionine-labeled HPIV3 was prepared (Wechsler et al., 1985) and used to analyse the effects of the compounds on adsorption and internalization of the virus in A549 cells as described previously (Bose et al., 2004; Zhao et al., 1996). Briefly, for the adsorption assay, 0.3 MOI of ^{35}S-HPIV3 (2.8×10^5 cpm) was added to chilled A549 cells in the presence of 13.75 μM of compounds. After 2 h of incubation at 4 °C

(the temperature that supports attachment but not internalization), the cells were washed extensively with chilled PBS. The washed cells were lysed with lysis buffer (50 mM Tris–HCl PH 8.0, 5 mM EDTA, 150 mM NaCl, 0.5% NP40) and the lysates radioactivity representing the attached ^{35}S-HPIV3 were counted with a liquid scintillation counter. For internalization assay, following attachment for 2 h in the absence of compounds at 4 °C, the cells were washed extensively with PBS and cultured in fresh Opti-MEM containing C5 or C7. The temperature was shifted to 37 °C to allow internalization of the attached virus. At 2 h post-internalization, cells were washed extensively with PBS and trypsinized with 0.25% trypsin-0.125% EDTA for 15 min at 37 °C to remove cell surface attached viruses. The protease activity was neutralized with complete DMEM and the cells were washed twice with PBS. The washed cells were lysed and the lysates representing the internalized ^{35}S-HPIV3 were counted with a liquid scintillation counter.

2.11. In vivo minigenome assay

In vivo HPIV3 minigenome assay was performed as described previously (Hoffman and Banerjee, 2000) with slight modifications. HeLa cell monolayers in 12-well plates, grown to 90% confluency, were infected with recombinant vaccinia virus vTF7-3, which expresses T7 RNA polymerase, at an MOI of 3. At 1 h PI, cells were washed with PBS and transfected with HPIV3 minigenome plasmid HPIV3-MG(–) (200 ng) carrying luciferase reporter gene together with supporting plasmids car-

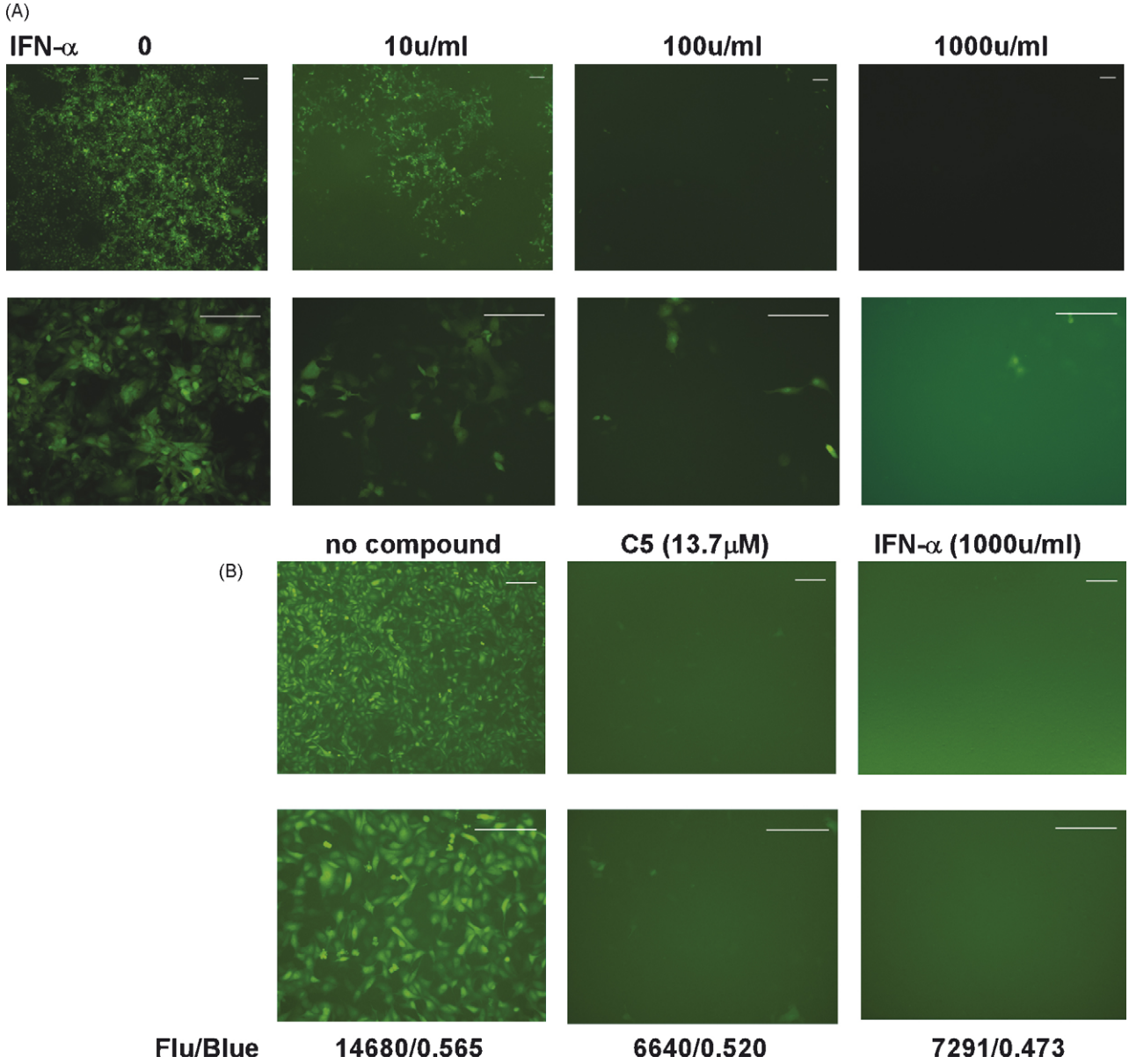

Fig. 1. The r-GFP-HPIV3 infected CV-1 cell-based screening system. (A) CV-1 cells were pretreated with increasing concentrations of IFN-α as indicated and were subsequently infected with r-GFP-HPIV3 at an MOI of 1. The photographs were taken at 24 h PI in two different magnifications. The scale bar represents 100 μm. (B) Effects of C5 on r-GFP-HPIV3 infection. The photographs were taken during screening. The corresponding values of fluorescence and blue staining are indicated below.

rying N (600 ng), P (750 ng) and L (100 ng) by using Lipofectin. After 5 h, transfection medium was removed, cells were washed with PBS and incubated in DMEM with different concentrations of C5 or C7, or only DMSO for 24 h. Cells were lysed in 150 μl of lysis buffer, from which 1.5 μl aliquots were used to determine luciferase activity in a luminometer (VICTOR) according to the manufacturer's instructions (Luciferase Assay Kit; Roche).

2.12. Primary transcription assay

The primary transcription assay was performed as described previously (Zhao et al., 1996). In brief, confluent A549 cells were cultured in the presence of anisomycin at 100 μM for 2 h. After 2 h, the media was removed and replaced with fresh Opti-MEM containing various concentrations of C5 or C7 as well as 100 μM of anisomycin. Then the cells were infected with HPIV3 at an MOI of 1. At 6 h PI, the cells were lysed and the total RNA was extracted for Northern blot.

3. Results

3.1. Development of a cell-based assay system using r-GFP-HPIV3 infected CV-1 cells and identification of "hits" from screening a small molecule library

A cDNA clone (pOCUS-PIV3-GFP) encoding the complete genome of the HPIV3 47885 strain with GFP inserted between P and M genes was constructed as described under Section 2. This position of insertion was chosen primarily due to its effective expression potential (Durbin et al., 2000; Sakai et al., 1999). The GFP gene contained an independent transcription unit with its own start gene (M start 37283737) and stop gene (P end 3599–3628). A total of 786 bp was inserted maintaining the required multiple of six (the rule of six), for transcription and replication of viruses belonging to the paramyxoviridae family (Durbin et al., 1997; Lamb and Kolakofsky, 1995). pOCUS-PIV3-GFP and the three supporting plasmids encoding the HPIV3 proteins NP, P and L were transfected into HeLa cells infected with vTF7-3 expressing T7-RNA polymerase. In the cell monolayer incubated with the clarified transfection supernatant, green syncytia were formed as viewed under fluorescence microscope, indicating that the r-GFP-HPIV3 was successfully recovered. The recovered r-GFP-HPIV3 was further purified and amplified in CV-1 cells, showing similar biological characteristics such as syncytia formation and plaque morphology in cultured cells as wild type HPIV3.

To evaluate the r-GFP-HPIV3 infected CV-1 cell-based assay for its sensitivity, quantifiability and reproducibility against antiviral agents, we first treated cells with IFN-α of 10 u/ml, 100 u/ml or 1000 u/ml for 16 h before infection and examined the GFP expression in cells under fluorescence microscope at 24 hPI. As shown in Fig. 1A, GFP expression in cells was reduced by IFN-α in a dose-dependent manner and virtually no fluorescence was observed for IFN-α of 1000 u/ml used as the positive control. To quantitate the intensity, the fluorescence was measured at excitation/emission wavelength of 485 nm/535 nm using a VICTOR Readout System. As shown in Fig. 1B, the fluorescence value in C5 treated cells (6640) was lower than background level (7473 ± 58 for the same plate) and that in IFN-α treated cells (7291), indicating 100% inhibition of GFP expression. Based on the fluorescence values obtained in negative (15 636 ± 1353 for untreated/infected control) and positive control wells (6 901 ± 74 for 1000 u/ml of IFN-α treated/infected CV-1 cells, 7 050 ± 97 for mock infected control), the Z′-value for the well-to-well variation was counted to be 0.51 (>0.5), suggesting acceptable reproducibility of the assay (Mason et al., 2004). The cytotoxicity of IFN-α was assessed in a parallel blue staining assay with no significant difference to the non-treated control. These results demonstrated that the r-GFP-HPIV3 infected-CV-1 cell assay system is reliable for screening of the small molecule library and could be adapted for high-throughput screening (HTS) assay, although it does not allow us to distinguish between infectious virus, DI particle production and production of virus parts.

The small molecule library supplied by the ChemBridge Corp. has been used extensively for a variety screens yielding promising results (Gudkov and Komarova, 2005; Gurova et al., 2005). Our initial screening of 3600 compounds yielded 7 primary "hits". Among them, C5 (Fig. 1B) and C7 were selected having the most potent inhibitory effect on r-GFP-HPIV3 infection. Moreover, C5 and C7 share similar structural feature as shown in Fig. 2. Based on pharmacophore analyses of the two "hits", we further screened a group of structural analogs of these

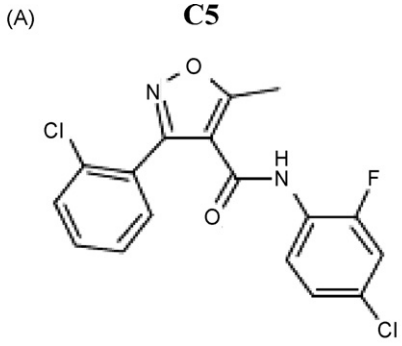

N-(4-chloro-2-fluorophenyl)-3-(2-chlorophenyl)-5-methyl-4-isoxazolecarboxamide

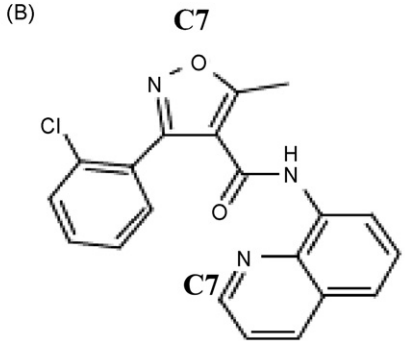

3-(2-chlorophenyl)-5-methyl-N-8-quinolinyl-4-isoxazolecarboxamide

Fig. 2. The molecular structures of C5 and C7.

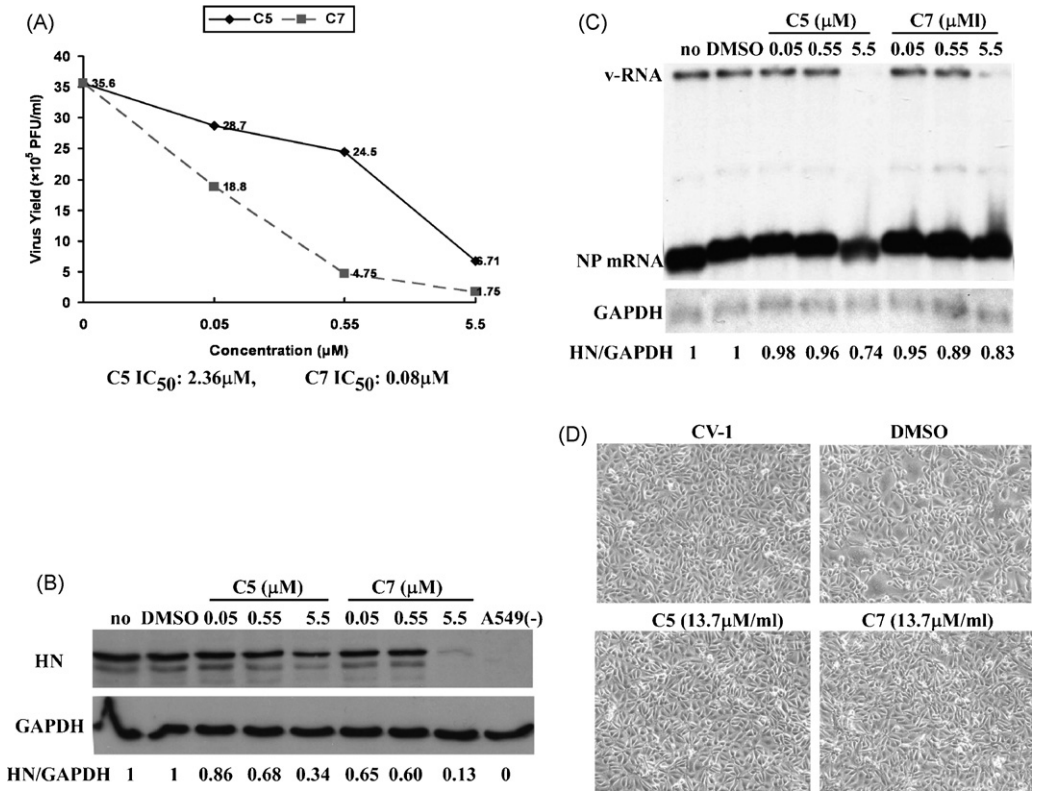

Fig. 3. Inhibition of wt-HPIV3 infection in cultured cells by C5 and C7. (A) A549 cells were infected with HPIV3 at an MOI of 0.3 in the presence of 0.05 μM, 0.55 μM, and 5.5 μM of C5 or C7. At 48 h PI, the cells were lysed and the supernatants were harvested and clarified for plaque assay as described in Section 2. Plaque assay was performed twice with similar results. A is a representative data. (B) At 24 h PI, the clarified supernatants were analysed by Western blot. "no", untreated/infected control; "DMSO", DMSO-treated/infected control; "A549 (–)", mock infected control. The NP proteins were quantified using the ImageQuant 5.2 and were normalized to the level of GAPDH proteins, which served as the loading control. The ratios of NP to GAPDH were calculated and shown below. (C) At 24 h PI, the cells were lysed for total RNA extraction for Northern blot analyses of HPIV3 N mRNA. Five μg of total RNA per sample were loaded and detected by hybridization using ^{32}P-random labeled NP-DNA probe. "no", untreated/infected control; "DMSO", DMSO-treated/infected control. The NP mRNAs were quantified using the ImageQuant 5.2 and were normalized to the level of GAPDH mRNAs, which served as the loading control. The ratios of NP to GAPDH were calculated and shown below. (D) CV-1 cells were infected with HPIV3 at an MOI of 0.3 in the presence of compounds at 13.7 μM or DMSO. The photographs were taken at 24 h PI.

two compounds identified in ChemBridge repository using a searchable database (http://www.hit2lead.com). Although less potent than C5 and C7, most of them also possessed antiviral properties against r-GFP-HPIV3 in culture (data not shown). These results strongly suggest that they belong to a novel group of HPIV3 inhibitors and further structure activity relationship (SAR) studies were needed to establish their usefulness as potential antivirals.

3.2. Inhibition of wild type HPIV3 infection in cultured cells

Since HPIV3 infects the epithelial cells of lung as the primary target, we used A549 cells that are widely used as a model for airway epithelia (Bose et al., 2001; Gao et al., 2001). To test the antiviral activity of C5 and C7, A549 monolayer was infected with HPIV3 at an MOI of 0.3 for 48 h in the presence of 0.05 μM, 0.55 μM or 5.5 μM of the two compounds. We found that, with the increase of the concentration of C5 and C7, both virus titers (Fig. 3A) and viral protein HN expression (Fig. 3B) in the supernatant concomitantly decreased as compared to untreated or DMSO-treated/infected samples. The viral RNA and the NP mRNA also decreased (Fig. 3C) in cells treated with C5 or C7 at the concentration of 5.5 μM. The IC_{50} for C5 and C7 to inhibit virus production (Fig. 3A) are 2.36 μM and 0.08 μM, respectively. These results indicate that C5 and C7 are efficient antiviral agents against HPIV3, C7 is more potent than C5, and their activity is manifested in a dose-dependent manner. However, like IFN, the compounds did not inhibit virus if added later in the infection (data not shown).

In addition, as shown in Fig. 3D, treatment of C5 or C7 (13.75 μM) rendered CV-1 cells less susceptible to HPIV3 infection as shown by the absence of extensive syncytia formation as compared to DMSO-treated/infected cells. These observations further confirmed the antiviral activity of these two primary "hits" against HPIV3 obtained from the small molecule library screening.

We next evaluated the antiviral potency of C5 and C7 against HPIV3 at an MOI of 0.3 with increased concentration of the compounds. We found the virus yield (Fig. 4A) and viral protein HN expression (Fig. 4B) were both further inhibited by C5 and C7 with the increase of their final concentrations. As shown in Fig. 4A, 27.5 μM of C5 was able to inhibit more than 98% of virus yield. But for C7, maximum inhibition of 94% occurred at 11 μM; increase of concentration did not inhibit further. To

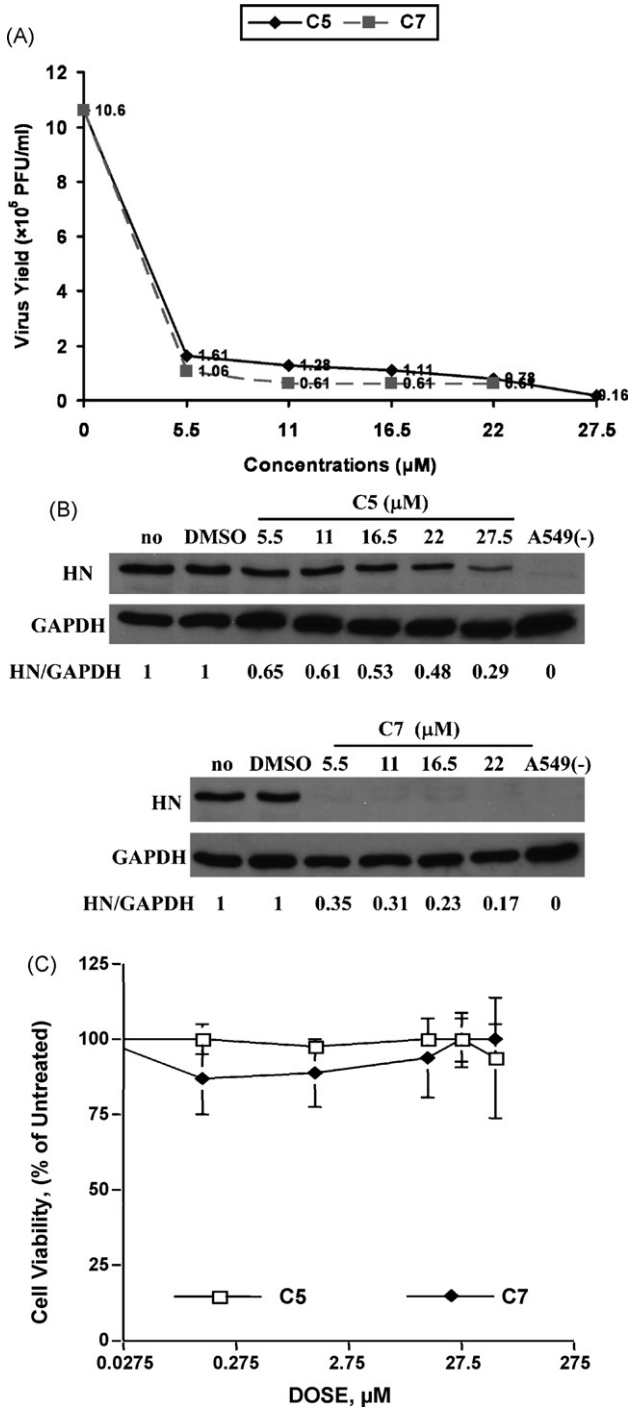

Fig. 4. The potency of C5 and C7 to inhibit HPIV3 in A549 cells (A) and (B). Dose-dependent inhibition of HPIV3 by C5 and C7. A549 cells were treated with indicated concentrations of C5 or C7 and were subsequently infected with HPIV3 at an MOI of 0.3. At 48 h PI, the cells were lysed and the supernatants were harvested and clarified for plaque assay (A) and Western blot analyses (B). (A) A representative plaque assay data. Plaque assay was performed twice with similar results. (B) "no", untreated/infected control; "DMSO", DMSO-treated/infected control; "A549 (–)", mock infected control. The NP proteins were quantified using the ImageQuant 5.2 and were normalized to the level of GAPDH proteins, which served as the loading control. The ratios of NP to GAPDH were calculated and shown below. C. MTT assay for evaluating the cytotoxicity of C5 and C7. C5 and C7 were added to A549 monolayers at various concentrations of 0.137 μM, 1.37 μM, 13.7 μM, 27.5 μM, and 55 μM as indicated. After 48 h, MTT assay was conducted as described in Section 2. Data for cell viability is presented as percentage of untreated control.

check the cytotoxicity of the two compounds at the higher concentrations, we performed MTT assay at 24 h, 48 h and 72 h post-treatment. Fig. 4C shows the one at 48 h post-treatment, which is corresponding to the time point for the detection of virus yield and HN protein expression shown in Fig. 4A and B. No apparent cytotoxicity was observed following the treatment of C5 or C7 at concentrations less than 27.5 μM at 48 h post-treatment.

3.3. Characteristics of the antiviral activity of C5 and C7 in A549 cells

To ascertain at which time period in the HPIV3 life cycle these compounds exert their inhibitory effect, A549 cells were treated with the compounds for 0–48 h, 0–2 h, or 2–48 h during infection. At 48 h PI, cells were lysed by freezing and thawing and the clarified supernatants were collected for plaque assay (Fig. 5A) and Western blot analyses (Fig. 5B). By comparing the viral yield in 2–48 h and 0–48 h treated samples for C5 or C7, the inhibitory effect was decreased by 9% although the treatment was delayed for only 2 h, suggesting that C5 and C7 must exert their antiviral activity in early period of HPIV3 life cycle. Because there was a noticeable decrease of virus

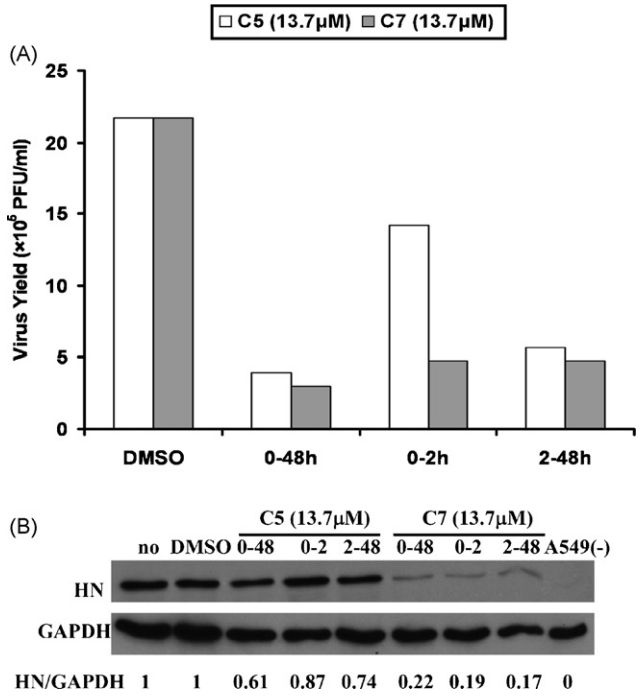

Fig. 5. Time course of inhibition of HPIV3 infection by C5 and C7. A549 cells were infected with HPIV3 at an MOI of 0.3 in the presence of 13.7 μM of C5 or C7 from 0 h to 24 h, 0 h to 2 h, or 2 h to 24 h during infection. Zero hours refers to the time when viruses were added. At 48 h PI, the cells were lysed and the supernatants were harvested and clarified for plaque assay (A) and Western blot analyses (B). (A) The plaque assay was performed twice with similar results. A representative data is shown. (B) "no", untreated/infected control; "DMSO", DMSO-treated/infected control; "A549 (–)", mock infected control. The NP proteins were quantified using the ImageQuant 5.2 and were normalized to the level of GAPDH proteins, which served as the loading control. The ratios of NP to GAPDH were calculated and shown below.

titer and HN protein expression during 0–2 h treatment with the compounds, especially for C7 (C5 is not nearly as potent when applied for 2 h and then removed), we wanted to ascertain whether adsorption and internalization of the virus were compromised. Using purified ^{35}S-HPIV3 as described in Section 2, we tested the adsorption and internalization processes using the standard biochemical procedures (Bose et al., 2004; Zhao et al., 1996). No significant difference of radioactivity between treated and untreated cells was found associated with the cells at 4 °C as well as within the cells when incubated at 37 °C for 2 h, strongly suggesting that the inhibitory effect is not directed at the steps of attachment and penetration in early life cycle of the virus. In addition, as indicated by the virus yield and viral HN expression in samples pretreated with the compounds for 2 h or 4 h, the pretreatment brings about increased antiviral effect during HPIV3 infection (data not shown), suggesting a possible prophylactic role of the compounds against HPIV3 infection.

3.4. Inhibition of primary transcription of HPIV3 by C5 and C7

To identify the step(s) in virus' life cycle where the observed inhibition occurs, we used the HPIV3 minigenome transcription system (Hoffman and Banerjee, 1997), in which a negative sense copy of the luciferase gene containing minigenome is made by T7 RNA polymerase and encapsidated within the cells following transfection of supporting plasmids encoding L, P, and N protein. Subsequently, the negative minigenome RNP is transcribed by virion-associated RNA polymerase (L and P) to produce a positive sense luciferase gene which is then quantitated by a luminometer measuring luciferase production. We cotransfected the HeLa cells with the minigenome cDNA pHPIV3-MG(–) and the supporting plasmids of N, P and L under optimal conditions. At 5 h post-transfection the media was replaced with fresh one containing C5 or C7 and the cells were lysed and collected for luciferase assay at 24 h post-transfection. The data (Fig. 6) demonstrated that the luciferase activity (transcription of viral genome) in cells treated with C5 or C7 decreased in a dose-dependent manner, as shown by the inhibition of luciferase expression measured by a luminometer and compared to DMSO-treated control. These results suggest that the antiviral effect of C5 and C7 is at viral transcriptional level possibly at the primary transcription step.

To test directly whether the inhibition by C5 and C7 is indeed at the primary transcription step, we used the protein inhibitor, anisomycin, to arrest protein synthesis in cells followed by infection with HPIV3 and measured the transcription level of the virus. The cells were infected with HPIV3 at an MOI of 1 in the presence of anisomycin (100 μM) as described in Materials and Methods. At 6 h PI, we extracted the total RNA from the cells for Northern blot analyses using ^{32}P labeled NP cDNA as probe. As shown in Fig. 7, although the level of viral genome RNA was same in different samples, as expected, the corresponding level of NP mRNA, however, decreased gradually with the increasing concentration of C5 (Fig. 7A) or C7 (Fig. 7B). The NP mRNAs were further quantitated using the ImageQuant 5.2 and were

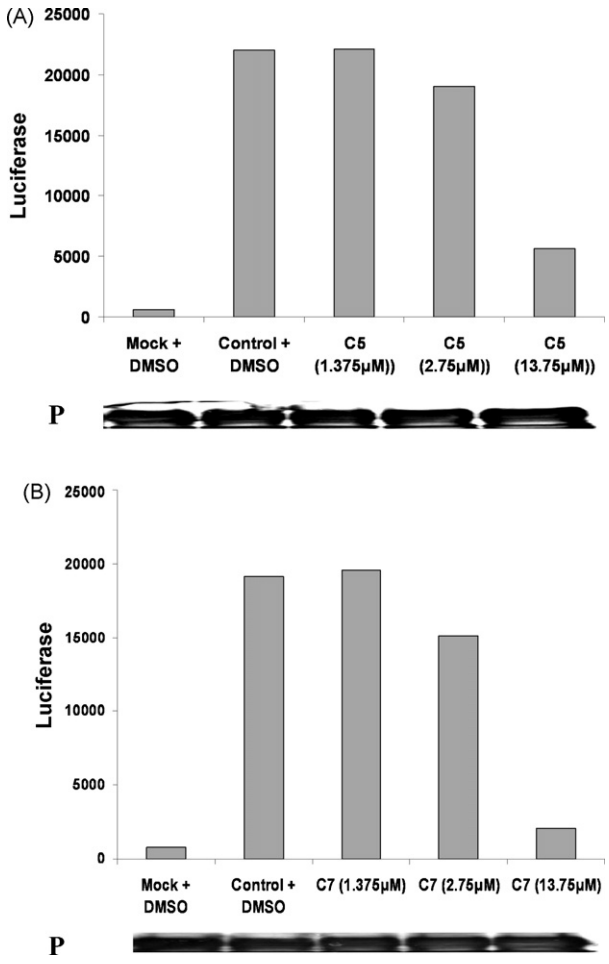

Fig. 6. Inhibition of viral transcription by C5 and C7 in HPIV3 minigenome system. In this system, a negative sense copy of the luciferase gene is transcribed to a positive one by viral RNA polymerase, which in turn encodes the luciferase for detection by a luminometer. HeLa cells were cotransfected with minireplicon cDNA pHPIV3-MG(–) and supporting plasmids of N, P and L. At 5 h post-transfection, indicated concentrations of C5 or C7 were added and at 24 h post-transfection cells were lysed and collected for luciferase assay. (A) and (B) show the effects of C5 and C7 on luciferase expression, respectively. The minigenome assay was performed three times with similar results. A representative data is shown. "mock + DMSO", transfected with N and P plasmids/DMSO treated control; "control + DMSO", transfected with N, P and L plasmids/DMSO treated control. The P protein expression was detected by Western blot and shown below.

normalized to the level of GAPDH mRNAs, which served as the loading control. The ratios of NP to GAPDH were calculated as shown below in the figure. In a parallel experiment, we treated A549 cell monolayer with indicated concentrations of C5 and C7, and subsequently infected the cells with HPIV3 at an MOI of 1. At 24 h PI, the supernatant for each sample was harvested for plaque assay (Fig. 7C) and Western blot analyses (data not shown). Data indicated that even against HPIV3 at an MOI of 1, C5 and C7 showed potent inhibitory activity, although less effectively compared to HPIV3 at an MOI of 0.3 (see Fig. 4A). Because the inhibition of virus yield parallels with that of mRNA production, it appears that C5 and C7 inhibited HPIV3 infection in A549 cells at the viral primary transcription level.

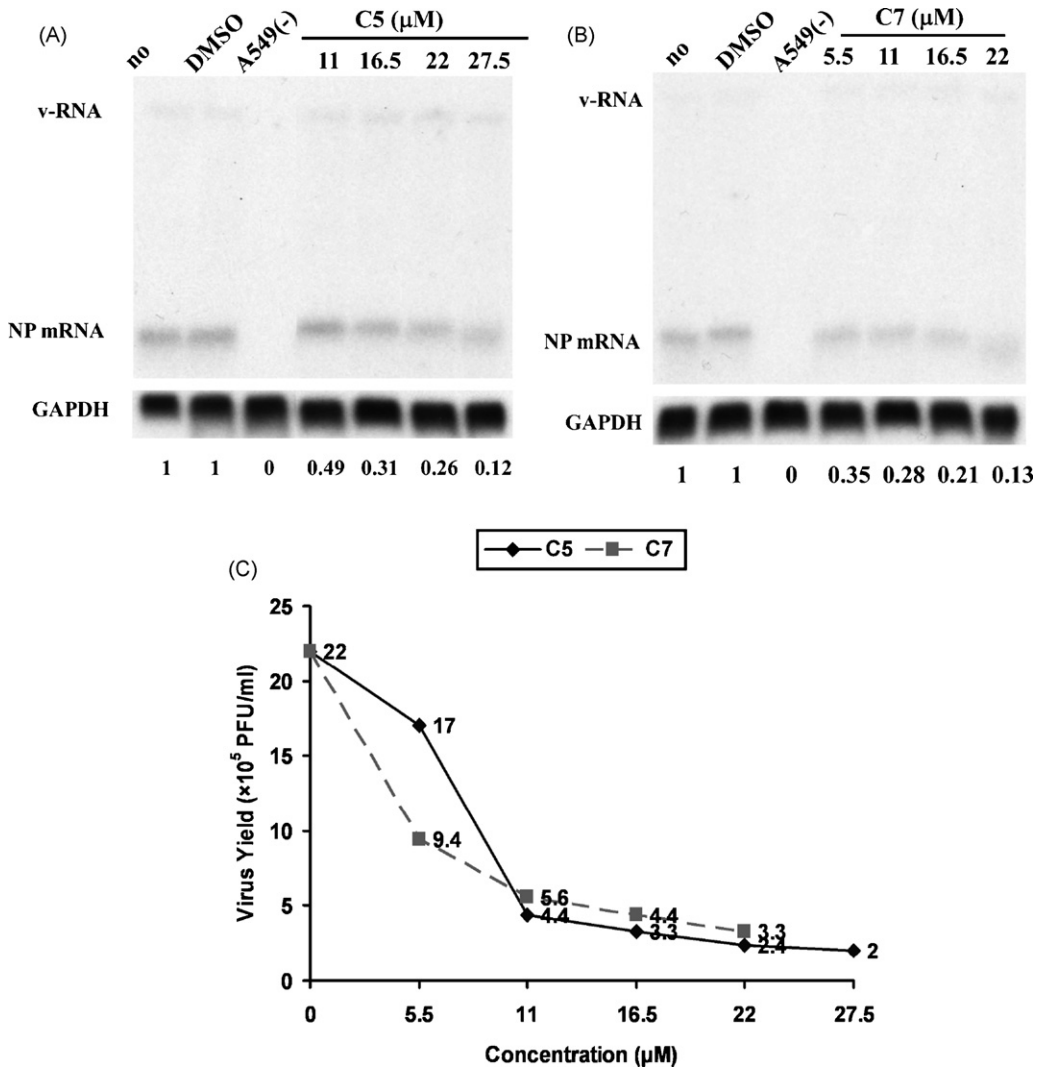

Fig. 7. Inhibition of wt-HPIV3 infection by C5 and C7 at the primary transcription level. (A) and (B). Northern blot analyses of viral primary transcripts. A549 cells were treated with indicated concentrations of C5 or C7 and were subsequently infected with HPIV3 at an MOI of 1 in the presence of the protein synthesis inhibitor, anisomycin, at 100 μM. At 6 h PI, the cells were lysed and the total RNA was harvested for Northern blot analysis using ^{32}P random labeled NP DNA as probe. The NP mRNAs were quantified using the ImageQuant 5.2 and were normalized to the level of GAPDH mRNAs, which served as the loading control. The ratios of NP to GAPDH were calculated and shown below. "no", untreated/infected control; "DMSO", DMSO-treated/infected control. (C) Plaque assay. A549 cells were infected with HPIV3 at an MOI of 1 in the presence of indicated concentrations of C5 and C7. At 24 h PI, the cells were lysed and the supernatants were harvested and clarified for plaque assay as described in Section 2. The plaque assay was performed twice with similar results. Here we show a representative data.

3.5. Specificity of the antiviral activity of C5 and C7

Since the mode of replication of HPIV3 primary transcription is similar to all viruses belonging to the order mononegavirales, we were interested to see whether C5 and C7 could inhibit another virus of the same order. We used vesicular stomatitis virus (VSV), a rhabdovirus, and studied the inhibition of its replication, if any, by C5 and C7. We treated CV-1 monolayer cells with Opti-MEM containing indicated concentrations of C5 or C7, and infected the cells with VSV at an MOI of 0.2. At 24 h PI, the cells treated with C5 and C7 appeared robust similar to mock infection control (Fig. 8A). Whereas the DMSO-treated/infected control showed extensive syncytia. These results strongly suggest that C5 and C7 could protect cells from the cytopathic effect of VSV infection. Consistent with this finding, the viral N protein expression (Fig. 8B) decreased in the compounds treated cells compared to the DMSO-treated/infected control. C5 and C7 had 19% and 58% inhibition, respectively, against VSV at 13.7 μM (Fig. 8B), whereas 35% and 65% inhibition, respectively, against HPIV3 at 5.5 μm (Fig. 4B), indicating relative effectiveness of the compounds towards HPIV3. We also carried out the same experiment using poliovirus, a picornavirus, no inhibition by the compounds was seen although guanidine-HCl, a known inhibitor of poliovirus, completely inhibited viral protein expression in polio-infected cells. Thus, C5 and C7 appear to be specific for the viruses belonging to mononegavirales order, possible also other members in paramyxovirus family, due to similarity in their mode of replication. The inhibition appears to be at the viral primary transcription level which is also a common fundamental biochemical step for this order of viruses.

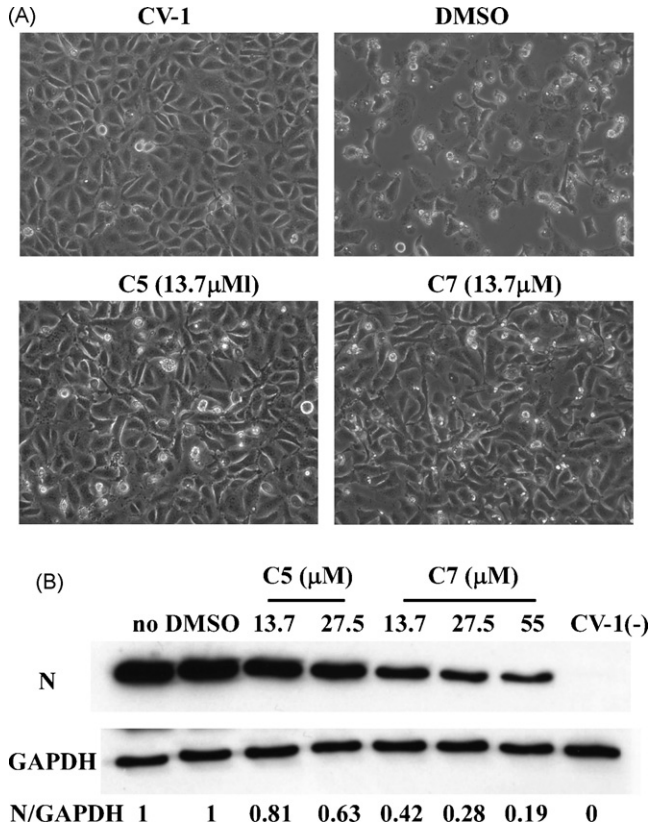

Fig. 8. Inhibition of VSV infection by C5 and C7. (A) CV-1 cells were infected with VSV at an MOI of 0.2 in the presence of C5 or C7 at 13.7 μM, or DMSO. At 24 h PI, the cells were examined under microscope. (B) Western blot analyses of VSV NP protein. CV-1 monolayers were infected with VSV ant an MOI of 0.2 in the presence of C5 or C7 at indicated concentrations. At 24 h PI, the cells were lysed and the supernatants were harvested and clarified for Western blot. "no", untreated/infected control; "DMSO", DMSO-treated/infected control; "CV-1 (–)", mock infected control. The NP proteins were quantified using the ImageQuant 5.2 and were normalized to the level of GAPDH proteins, which served as the loading control. The ratios of NP to GAPDH were calculated and shown below.

4. Discussion

HPIV3 is second only to respiratory syncytial virus (RSV) for acute lower respiratory tract disease for infants and children. Unfortunately so far effective vaccines or antivirals to combat HPIV3 infection are unavailable. Consequently the development and use of antiviral drugs capable of preventing or abrogating HPIV3 infection becomes a strong alternative approach. In the recent past antiviral discovery programs have been initiated towards targeting many pathogenic viruses using various mechanism-based screening methods (Hwang et al., 2003; Mason et al., 2004). Random chemicals and natural product mixtures are being tested for their ability to block replication of a variety of viruses in cell culture systems. Promising molecules, referred to as "hits" are systematically modified to reduce toxicity or increase biological half-life. We have used a fluorescence-based cell system to screen a library of small molecules for antiviral activity towards HPIV3. A pilot small-scale screening was performed on 3600 small molecules from the ChemBridge Diver set of 34,000 small molecules for initial screening using a recombinant HPIV3 expressing GFP.

We inserted the GFP gene into P–M junction of the full-length cDNA of HPIV3 (47885 strain). Recombinant HPIV3-GFP was produced which effectively infected HeLa, CV-1 and A549 cells producing expected, visible green color syncytia which were subsequently quantitated by fluorescence microscope and measured at 535 nm wavelength. The recombinant HPIV3-GFP virus (r-GFP-HPIV3) can be cultured and propagated in the same fashion as biologically derived virus, with some differences. It grew slower in CV-1 cells with the size of the plaques smaller than the wild type virus. The latter phenotype was previously observed for recombinant HPIV3 from the full-length infectious cDNA (Hoffman and Banerjee, 1997). However, another group recently reported recombinant HPIV3-GFP replicated with efficiency similar to that of wild type recombinant virus (Zhang et al., 2005). The discrepancy may be due to the different strain of virus (strain JS) used in their study or because they compared the recombinant HPIV3-GFP virus with the wild type recombinant virus only and not with the biologically derived virus.

We performed plaque assay, Western blot and Northern blot analyses to test the virus, viral protein and viral mRNA in HPIV3 infected cells in the presence or absence of the compounds. The two compounds C5 and C7 identified from initial screening of 3600 small molecules have significant antiviral properties against HPIV3 infection (Figs. 3–7). Except for preventing the cytopathic effect caused by HPIV3, C5 and C7 achieved IC_{50} values of 2.36 μM and 0.08 μM, respectively as determined by plaque assay (Fig. 3), even more effective than ribavirin, for which EC_{50} for inhibition of HPIV3 infectious virus production is 17.2 ± 6.9 μg/ml (70.4 ± 28.3 μM)(Leyssen et al., 2005), and hemagglutinin-neuraminidase inhibitors (Alymova et al., 2004) with the IC_{50} ranging from 0.7 μM to 11.5 μM. It is interesting to note that two compounds bear structural similarities (Fig. 2) indicating that their mode of action could be similar. In fact, we were able to obtain from the library several analogues of the compounds with similar antiviral property. Additional analogues could be custom synthesized based on computer prediction for increased potency of C5 and C7. Such work is currently underway. Subsequent series of studies unfolded that 2–4 h prior treatment of cells with the compounds resulted in increased inhibition of the virus suggesting a possible prophylactic role of the antiviral compounds.

Since the life-cycle of HPIV3 includes adsorption and entry, primary transcription followed by genome replication, virion assembly and release, we then determined which step(s) in the virus's life-cycle is possibly compromised by the action of the compounds. Our preliminary results indicated that adsorption and entry were not affected by the compounds. HPIV3 minigenome transcription assay in the cells clearly suggested that the compounds act at the viral transcription level (Fig. 6), and was subsequently confirmed to act at the primary transcription step following entry (Fig. 7). This finding is similar to the effect of IFN on HPIV3 infection in particular (Gao et al., 2001; Zhao et al., 1996) and viruses belonging to this family in general (Gotoh et al., 2001, 2002). Although the IFN-induced putative cellular component(s) involved in this inhibition process is not

known, it is possible that the putative factor interacts with L, NP, or P present in the input RNP. Alternatively, the antiviral compounds C5 and C7 may directly interact with these viral proteins or subvert specific interactions between the viral proteins or viral and host protein in the cells during the minigenome assay and HPIV3 infection (Figs. 6 and 7). The role of the compounds, if any, during L–P, N–P, or L–N–P interaction in the cells can be tested by standard immunoprecipitation using plasmid-expressed proteins. Recently, Luizzi et al. (Liuzzi et al., 2005), have shown that similar small molecules, that are structurally different from C5 and C7 inhibited RSV replication. The compounds, identified by HTS assay (Mason et al., 2004), appear to block synthesis of RSV mRNA apparently by inhibiting guanylylaion of viral transcripts. These findings combined with our findings underscore the importance for the use of small molecule inhibitors that target various steps in the life-cycle of viruses in the family of paramyxoviridae.

Finally, the compounds appear to be effective also for VSV, a member of the same order of HPIV3 (Fig. 8), suggesting that they could be effective for RSV, measles, rabies and others, where no effective antiviral has been developed.

In conclusion, the in vitro study demonstrates that the r-GFP-HPIV3 infected cell-based assay is a very useful approach to screen antiviral agents against HPIV3 which may eventually be adapted for HTS system. The two potent inhibitors C5 and C7, identified from a library of small molecules, could be promising candidates for antiviral therapy as well as useful research tools for HPIV3 infection.

Acknowledgements

We thank Anatoliy Prokvolit and Mikhail Chernov, Department of Molecular Genetics, Cleveland Clinic Foundation, for supplying and screening the small molecular library. This work was supported by a grant from United States Public Health Services (to A.K.B.)

References

Alymova, I.V., Taylor, G., Takimoto, T., Lin, T.H., Chand, P., Babu, Y.S., Li, C., Xiong, X., Portner, A., 2004. Efficacy of novel hemagglutinin-neuraminidase inhibitors BCX 2798 and BCX 2855 against human parainfluenza viruses in vitro and in vivo. Antimicrob. Agents Chemother. 48, 1495–1502.

Belshe, R.B., Newman, F.K., Tsai, T.F., Karron, R.A., Reisinger, K., Roberton, D., Marshall, H., Schwartz, R., King, J., Henderson, F.W., Rodriguez, W., Severs, J.M., Wright, P.F., Keyserling, H., Weinberg, G.A., Bromberg, K., Loh, R., Sly, P., McIntyre, P., Ziegler, J.B., Hackell, J., Deatly, A., Georgiu, A., Paschalis, M., Wu, S.L., Tatem, J.M., Murphy, B., Anderson, E., 2004. Phase 2 evaluation of parainfluenza type 3 cold passage mutant 45 live attenuated vaccine in healthy children 6–18 months old. J. Infect. Dis. 189, 462–470.

Bose, S., Banerjee, A.K., 2002. Role of heparin sulfate in human parainfluenza virus type 3 infection. Virology 298 (1), 73–83.

Bose, S., Malur, A., Banerjee, A.K., 2001. Polarity of human parainfluenza virus type 3 infection in polarized human lung epithelial A549 cells: role of microfilament and microtubule. J. Virol. 75, 1984–1989.

Bose, S., Basu, M., Banerjee, A.K., 2004. Role of nucleolin in human parainfluenza virus type 3 infection of human lung epithelial cells. J. Virol. 78, 8146–8158.

Choudhary, S., Gao, J., Leaman, D.W., De, B.P., 2001. Interferon action against human parainfluenza virus type 3: involvement of a novel antiviral pathway in the inhibition of transcription. J. Virol. 75, 4823–4831.

Cortez, K.J., Erdman, D.D., Peret, T.C.T., Gill, V.J., Childs, R., Barrett, A.J., Bennett, J.E., 2001. Outbreak of human parainfluenza virus 3 infectious in a hematopoietic stem cell transplant population. J. Infect. Dis. 184, 1093–1097.

Durbin, A.P., Karron, R.A., 2003. Karron. Progress in the development of respiratory syncytial virus and parainfluenza virus vaccines. Clin. Infect. Dis. 37, 1668–1677.

Durbin, A.P., Siew, J.W., Murphy, B.R., Collins, P.L., 1997. Minimum protein requirements for transcription and RNA replication of a minigenome of human parainfluenza virus type 3 and evaluation of the rule of six. Virology 234, 74–83.

Durbin, A.P., Skiadopoulos, M.H., McAuliffe, J.M., Riggs, J.M., Surman, S.R., Collins, P.L., Murphy, B.R., 2000. Human parainfluenza virus type 3 (PIV3) expressing the hemagglutinin protein of measles virus provides a potential method for immunization against measles virus and PIV3 in early infancy. J. Virol. 74, 6821–6831.

Gao, J., De, B.P., Han, Y., Choudhary, S., Ransohoff, R., Banerjee, A.K., 2001. Human parainfluenza virus type 3 inhibits gamma interferon-induced major histocompatibility complex class II expression directly and by inducing alpha/beta interferon. J. Virol. 75, 1124–1131.

Gotoh, B., Komatsu, T., Takeuchi, K., Yokoo, J., 2001. Paramyxovirus accessory proteins as interferon antagonists. Microbiol. Immunol. 45 (12), 787–800.

Gotoh, B., Komatsu, T., Takeuchi, K., Yokoo, J., 2002. Paramyxovirus strategies for evading the interferon response. Rev. Med. Virol. 12 (6), 337–357.

Gudkov, A.V., Komarova, E.A., 2005. Prospective therapeutic applications of p53 inhibitors. Biochem. Biophys. Res. Commun. 331, 726–736.

Gurova, K.V., Hill, J.E., Guo, C., Prokvolit, A., Burdelya, L.G., Samoylova, E., Khodyakova, A.V., Ganapathi, R., Ganapathi, M., Tararova, N.D., Bosykh, D., Lvovskiy, D., Webb, T.R., Stark, G.R., Gudkov, A.V., 2005. Small molecules that reactivate p53 in renal cell carcinoma reveal a NF-kappaB-dependent mechanism of p53 suppression in tumors. Proc. Natl. Acad. Sci. U.S.A. 102, 17448–17453.

Heilman, C.A., 1990. Respiratory syncytial and parainfluenza viruses. J. Infect. Dis. 161, 402–406.

Hoffman, M.A., Banerjee, A.K., 1997. An infectious clone of human parainfluenza virus type 3. J. Viral. 71, 4272–4277.

Hoffman, M.A., Banerjee, A.K., 2000. Precise mapping of the replication and transcription promoters of human parainfluenza virus type 3. Virology 269, 201–211.

Hwang, S., Tamilarasu, N., Kibler, K., Cao, H., Ali, A., Ping, Y.H., Jeang, K.T., Rana, T.M., 2003. Discovery of a small molecule Tat-trans-activation-responsive RNA antagonist that potently inhibits human immunodeficiency virus-1 replication. J. Biol. Chem. 278, 39092–39103.

Kunkel, T.A., 1985. Rapid and efficient site-specific mutagenesis without phenotypic selection. Proc. Natl. Acad. Sci. U.S.A. 82, 488–492.

Lamb, R.A., Kolakofsky, D., 1995. Paramyxoviridae: the viruses and their replication. In: Fields, B.N., Knipe, D.M., Howley, P.M. (Eds.), Fields Virology. Lippincott-Raven, NY, p. 1307.

Leyssen, P., Balzarini, J., De Clercq, E., Neyts, J., 2005. The predominant mechanism by which ribavirin exerts its antiviral activity in vitro against flaviviruses and paramyxoviruses is mediated by inhibition of IMP dehydrogenase. J. Virol. 79, 1943–1947.

Liuzzi, M., Mason, S.W., Cartier, M., Lawetz, C., McCollum, R.S., Dansereau, N., Bolger, G., Lapeyre, N., Gaudette, Y., Lagace, L., Massariol, M.J., Do, F., Whitehead, P., Lamarre, L., Scouten, E., Bordeleau, J., Landry, S., Rancourt, J., Fazal, G., Simoneau, B., 2005. Inhibitors of respiratory syncytial virus replication target cotranscriptional mRNA guanylylation by viral RNA-dependent RNA polymerase. J. Virol. 79, 13105–13115.

Madhi, S.A., Ramasamy, N., Petersen, K., Madhi, A., Klugman, K.P., 2002. Severe lower respiratory tract infections associated with human parainfluenza viruses 1–3 in children infected and noninfected with HIV type 1. Eur. J. Clin. Microbiol. Infect. Dis. 21, 499–505.

Mansfield, M.A., Mabuchi, M., MacDonald, C.G., Pluskal, M.G., 1999. Immobilon-Ny+ nucleic acid blotting membrane: an advanced nylon mem-

brane optimized for superior fixation and reprobing. Biotechniques 27, 1253–1257.

Mason, S.W., Lawetz, C., Gaudette, Y., Do, F., Scouten, E., Lagace, L., Simoneau, B., Liuzzi, M., 2004. Polyadenylation-dependent screening assay for respiratory syncytial virus RNA transcriptase activity and identification of an inhibitor. Nucleic Acids Res. 32, 4758–4767.

Moscona, A., 2005. Entry of parainfluenza virus into cells as a target for interrupting childhood respiratory disease. J. Clin. Invest. 115, 1688–1698.

Murphy, B.R., 1988. Current approaches to the development of vaccines effective against parainfluenza viruses. Bull. World Health Org. 66, 391–397.

Neznanov, N., Chumakov, K.M., Neznanova, L., Almasan, A., Banerjee, A.K., Gudkov, A.V., 2005. Proteolytic cleavage of the p65-RelA subunit of NF-κB during poliovirus infection. J. Biol. Chem. 280, 24153–24158.

Pastey, M.K., Gower, T.L., Spearman Jr., P.W., Growe, J.E., Graham, B.S., 2000. A RhoA-derived peptide inhibits syncytium formation induced by respiratory syncytial virus and parainfluenza virus type 3. Nat. Med. 6, 35–40.

Reed, G., Jewett, P.H., Thompson, J., Tollefson, S., Wright, P.F., 1997. Epidemiology and clinical impact of parainfluenza virus infections in otherwise healthy infants and young children <5 years old. J. Infect. Dis. 175, 807–813.

Sakai, Y., Kiyotani, K., Fukumura, M., Asakawa, M., Kato, A., Shioda, T., Yoshida, T., Tanaka, A., Hasegawa, M., Nagai, Y., 1999. Accommodation of foreign genes into the Sendai virus genome: sizes of inserted genes and viral replication. FEBS Lett. 456, 221–226.

Tanaka, Y., Kato, J., Kohara, M., Galinski, M.S., 2006. Antiviral effects of glycosylation and glucose trimming inhibitors on human parainfluenza virus type 3. Antiviral. Res. 72, 1–9.

Wechsler, S.L., Lambert, D.M., Galinski, M.S., Heineke, B.E., Lambert, A.L., Mink, M., Rochovansky, O.M., Pons, M.W., 1985. A simple method for increased recovery of purified paramyxovirus virions. J. Virol. Methods 12, 179–182.

Yuan, J., Cheung, P.K., Zhang, H., Chau, D., Yanagawa, B., Cheung, C., Luo, H., Wang, Y., Suarez, A., McManus, B.M., Yang, D., 2004. A phosphorothioate antisense oligodeoxynucleotide specifically inhibits coxsackievirus B3 replication in cardiomyocytes and mouse hearts. Lab. Invest. 84, 703–714.

Zhang, L., Bukreyev, A., Thompson, C.I., Watson, B., Peeples, M.E., Collins, P.L., Pickles, R.J., 2005. Infection of ciliated cells by human parainfluenza virus type 3 in an in vitro model of human airway epithelium. J. Virol. 79, 1113–1124.

Zhao, H., De, B.P., Das, T., Banerjee, A.K., 1996. Inhibition of human parainfluenza virus-3 replication by interferon and human MxA. Virology 220, 330–338.